Hindawi Publishing Corporation
Physics Research International
Volume 2014, Article ID 872381, 7 pages
http://dx.doi.org/10.1155/2014/872381

Research Article

Electronic Transport Properties of Doped C_{28} Fullerene

Akshu Pahuja and Sunita Srivastava

Department of Physics, Panjab University, Chandigarh 160014, India

Correspondence should be addressed to Akshu Pahuja; akshuh@yahoo.com

Received 21 August 2014; Revised 19 October 2014; Accepted 11 November 2014; Published 26 November 2014

Academic Editor: Yuan Ping Feng

Endohedral doping of small fullerenes like C_{28} affects their electronic structure and increases their stability. The transport properties of Li@C_{28} sandwiched between two gold surfaces have been calculated using first-principles density functional theory and nonequilibrium Green's function formalism. The transmission curves, IV characteristics, and molecular projected self-consistent Hamiltonian eigenstates of both pristine and doped molecule are computed. The current across the junction is found to decrease upon Li encapsulation, which can be attributed to change in alignment of molecular energy levels with bias voltage.

1. Introduction

The last few decades of the twentieth century witnessed an upsurge in development of electronics based on molecular devices [1]. Electrical measurements on single molecules embedded between electrodes have attracted special attention [2–5]. Electron transport across such molecular junctions gives rise to interesting phenomena like negative differential resistance, rectification, single electron characteristics [5–7], and so forth. This has resulted in their application as field effect transistors [8], logic gates [9], switches [10], and sensors [11]. Numerous attempts have been made to investigate transport properties of a fullerene molecule [12–14]. A fullerene molecule possesses unique structural and electronic properties, and its role as a functional electronic device [15, 16] has been widely analyzed. The transport properties of a fullerene molecule are influenced by its orientation between the electrodes [17], the nature of contact with the electrodes [18], and also on the type of doping and nature of dopant [19, 20]. An et al. found that insertion of Li into C_{20} cage improves its transmission capacity and increases the equilibrium conductance by about 66.67% [21]. Zhang et al. revealed that the conductivity for the doped C_{60} fullerene is higher than that of the pristine fullerene [22].

The spin-resolved transport properties of C_{28} molecule sandwiched between Au electrodes with different contact configurations have been examined theoretically [14]. C_{28} is the smallest fullerene that has been found to be experimentally significant [23, 24]. Since C_{28} molecule is very active, it can form particularly stable endohedral complexes [25–27]. Guo et al. found that empty C_{28} fullerene behaves as a hollow tetravalent superatom with tetrahedral symmetry [28]. It was proposed that metals with electronegativities smaller than 1.54 should form endohedral fullerenes larger than a minimum size, which depends on the radius of the trapped atom. Based on the above size and electronegativity considerations, it should be possible to encapsulate Li atom in C_{28} cage. Insertion of Li atom in a smaller fullerene molecule has been found to increase its conductivity [21], and also endohedral derivatives of fullerene molecules based on Li have been investigated [29, 30]. In this work we undertake the study of transport properties of endohedral fullerene Li@C_{28} sandwiched between Au (111) electrodes using a first-principles computational method based on density functional theory in combination with nonequilibrium Green's function theory. Doping can effectively change the electronic properties of fullerenes and hence provides an opportunity to modify transport properties as well. Thus we attempt to understand the effect of single-atom change on transport properties of C_{28} fullerene. The transmission spectra at different bias voltage and IV characteristics are plotted and compared for both pure and doped C_{28} molecules.

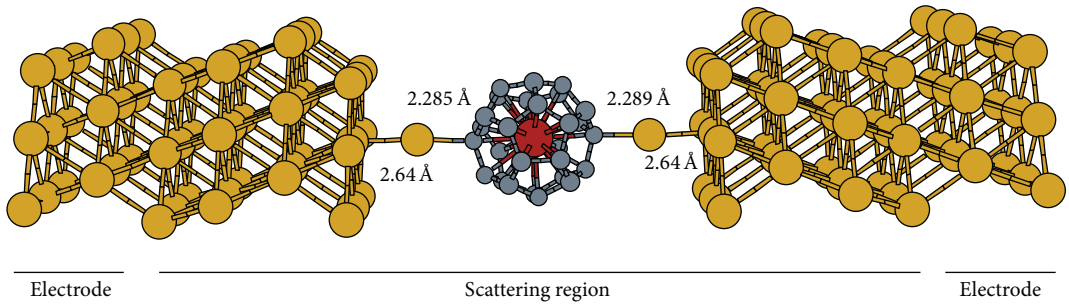

Figure 1: The geometry of the two-probe system Au-Li@C_{28}-Au. The fullerene molecule is coupled to two semi-infinite Au (111) electrodes through Au adatoms. The scattering region includes a portion of semi-infinite electrodes.

2. Computational Details

The geometry relaxations and electronic structure calculations for both Li@C_{28} and C_{28} molecules are performed based on DFT formulism using SIESTA [31] package with LDA functional in Ceperley and Alder form [32]. A SZP basis set is employed to describe the localized atomic orbitals. The core electrons are modeled with Troullier and Martins [33] nonlocal pseudopotential. An energy cutoff for real-space mesh size is set to be 400 Ry. All atomic positions are fully relaxed with a force tolerance of 0.04 eV/Å. For the analysis of electron transport through the molecular contact we used the TRANSIESTA [34] code, which implements the NEGF formalism for the single-particle Kohn-Sham Hamiltonian obtained from DFT calculations performed with SIESTA.

The current through the atomic scale system is calculated from Landauer-Büttiker [35] formula:

$$I = \frac{e}{h}\int_{-\infty}^{\infty} T(E,V)\left[f(E-\mu_1) - f(E-\mu_2)\right]dE, \quad (1)$$

where μ_1 and μ_2 are the electrochemical potentials of the left and right electrodes, V is the external bias, and $f(E)$ is the Fermi-Dirac distribution function. $T(E,V)$ is the transmission coefficient at energy E and bias voltage V and represents the quantum mechanical transmission probability for electrons. Consider

$$\mu_{1,2} = E_f \pm \frac{eV}{2}. \quad (2)$$

The energy region between μ_1 and μ_2, which contributes to the current integral above, is referred to as the bias window. A sample of $3 \times 3 \times 30$ k-points for computing transport properties was employed by the method of Monkhorst-Pack [36] to describe the Brillouin zone.

The system under study can be divided into three parts: left electrode, right electrode, and the scattering region, which includes the fullerene molecule and a few atomic layers of the electrodes. C_{28} molecule is rigidly attached to Au (111) surface by first positioning it between the two surfaces such that it has a desirable Au–C bonding distance 0.225 nm and then relaxing the whole system until the forces on all atoms are less than 0.04 eV/Å. Two Au adatoms in the right and left electrodes are adopted for effective coupling with electrodes due to the small C_{28} molecular radius. After structural relaxation, the equilibrium Au–C distances become 2.285 Å and 2.289 Å, respectively, for the left and right electrodes. The distance between Au adatom and the nearest neighboring Au atom of Au (111) surface is about 2.64 Å (Figure 1).

3. Results and Discussion

3.1. Structures of Pristine and Doped C_{28} Molecules. The ground-state structure of C_{28} molecule has T_d symmetry with three unique carbon atoms. The three C–C bond lengths R_1, R_2, and R_3 in the relaxed structure are 1.477, 1.575, and 1.457 Å, respectively (as shown in Figure 2). The binding energy is calculated to be 8.42 eV. These values agree well with the previous reports [37]. The endohedral atom was placed at the centrosymmetric position inside the cage and the structure was allowed to relax. It was observed that the dopant occupies the central position, maintaining the overall tetrahedral symmetry of the cage. An elongation in bond lengths as a result of the expansion of the cage is observed.

C_{28} molecule is known to have a small band gap. However, it is found that, as a result of insertion of Li, its HOMO-LUMO gap reduces further from 0.326 to 0.143 eV, and therefore it is expected that it should have a higher equilibrium conductance (i.e., transmission coefficient at the Fermi energy of the system). The electronic energy levels of C_{28} and Li@C_{28} molecules near Fermi level are illustrated in Figure 3. Both HOMO and LUMO levels move closer to the Fermi level as a result of doping with Li, thus decreasing the energy difference between these levels.

3.2. Transport Properties under Zero Bias. Transmission function is the most important physical quantity for determining electron transport through single molecular junctions. The zero bias transmission functions for pure C_{28} molecule and Li@C_{28} systems in the energy range of −1 to 1 eV have been shown in Figures 4(a) and 4(d), respectively; the Fermi level has been shifted to zero for clarity. The equilibrium conductance of the system can be computed as $G = G_0 T(E_f)$, where $G_0 = 2e^2/h$. It is found that zero bias conductance for the junction formed by C_{28} is $0.935G_0$ and that of Li@C_{28} is $0.311G_0$, respectively.

For the molecular junction formed by C_{28}, there are two transmission peaks near the Fermi level, which contribute to

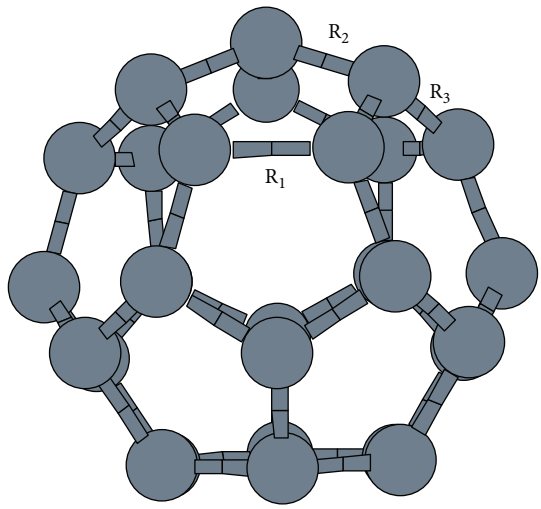

Figure 2: The optimized geometry of C_{28} molecule after structural relaxation. R_1 is used for bond between base atoms in pentagon, R_2 is a bond to the apex atom of the pentagon, and R_3 is for the hexagon bond.

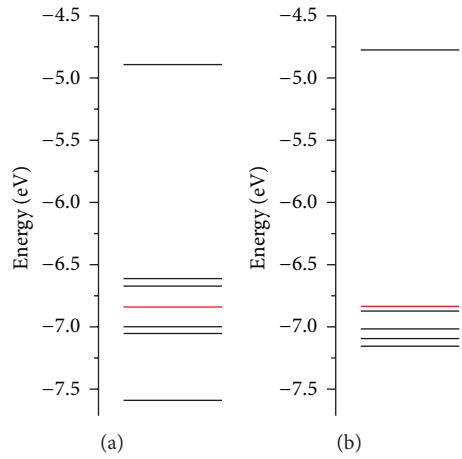

Figure 3: The energy level diagram of isolated (a) C_{28} (b) Li@C_{28} molecules. The position of Fermi level is indicated by red lines.

transport of electrons across the junction. However, in Figure 4(d), it is found that, as a result of Li doping, there is a shift in molecular orbitals as a transmission valley is developed near the Fermi level. Hence the zero bias conductance for Li@C_{28} is less as compared to the undoped molecule even though the band gap of the isolated C_{28} molecule is found to decrease upon endohedral doping with Li. This is mainly because the electronic transport depends on several factors, such as the broadening of the energy levels of the central cluster, the alignment of the Fermi level of the electrodes within the HOMO-LUMO gap, charge transfer between the electrodes and the central cluster, and so forth.

The molecular projected self-consistent Hamiltonian (MPSH) eigenstates near Fermi level for both devices are shown in Figure 5, which are the perturbed molecular orbitals due to coupling between molecule and the electrodes. The calculated results show that, under zero bias voltage, the HOMO of C_{28} is very close to the Fermi level, so the HOMO mostly contributes to the equilibrium conductance. For Li@C_{28} the projected HOMO-LUMO gap increases, which can be attributed to coupling with electrodes. This leads to a lower value of equilibrium conductance. In both cases it is the HOMO that contributes to conduction, more than the LUMO.

The HOMO and LUMO of C_{28} and Li@C_{28} are plotted in Figure 6. It is known that the charge density distribution of molecular orbitals affects the transport of electrons. The charge distribution of HOMO is clearly different for both cases. It can be observed that the molecular orbitals for C_{28} are more delocalized in character, which indicates stronger molecule-electrode interaction. Additionally, the charge density for HOMO is more in case of C_{28} and is also aligned along the transmission axis (z-axis).

3.3. Transport Properties under Finite Bias. The transport behavior of a molecular junction can be modulated by applying a bias voltage. Therefore we investigate the effect

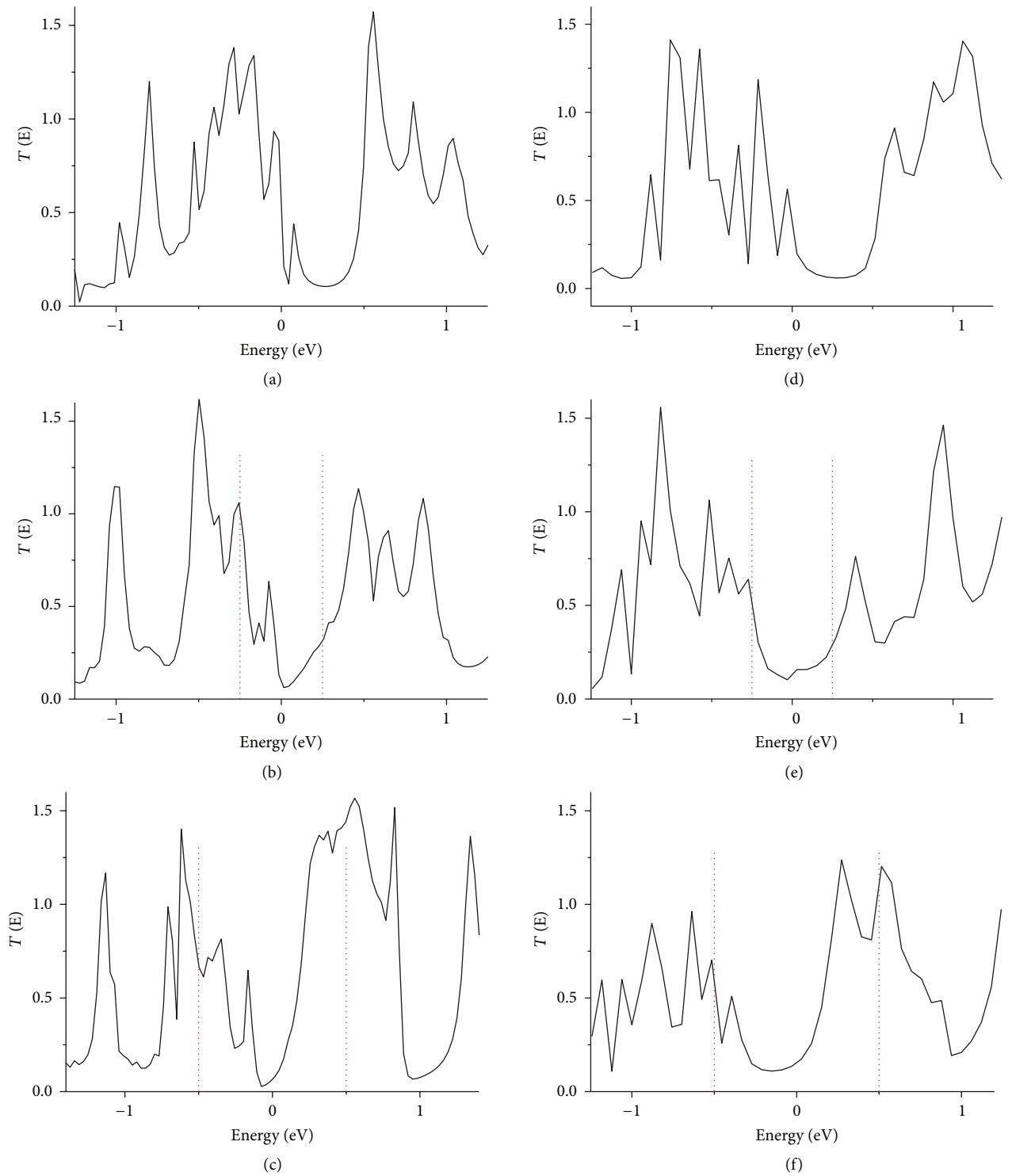

FIGURE 4: The transmission as a function of energy around the Fermi energy (here set to zero) of a C_{28} molecule at bias voltages (a) 0 V, (b) 0.5 V, and (c) 1 V and Li@C_{28} at bias voltages (d) 0 V, (e) 0.5 V, and (f) 1 V. The bias window is shown by dotted lines.

of applied bias in both directions. The electron transport across a junction and hence the current flow depend on the extent of coupling between molecule and electrodes. Strong coupling will aid transfer of electrons and hence a stronger peak will appear in transmission spectra. On the other hand, a vanishing transmission near the Fermi region indicates weakening of electronic transport.

For C_{28}, at a bias voltage of 0.5 V (Figure 4(b)), a diffusive transmission peak appears in the bias window just below the Fermi level, which contributes to current flow. In general,

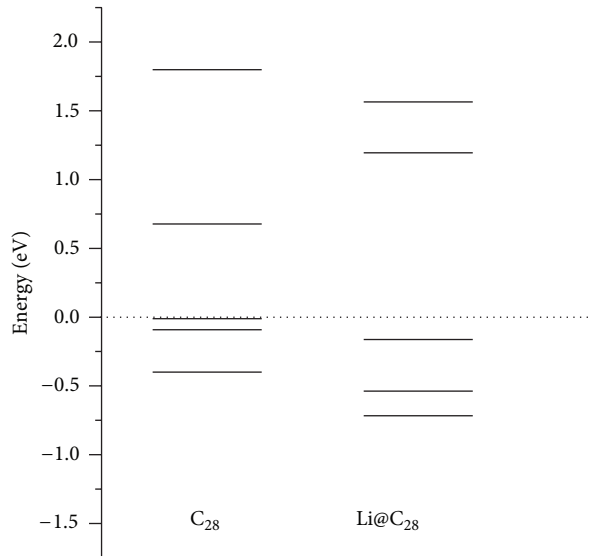

Figure 5: The projected Hamiltonian spectra of C_{28} and $Li@C_{28}$ in the two-probe system. The position of Fermi level is indicated by the dotted line at 0 eV.

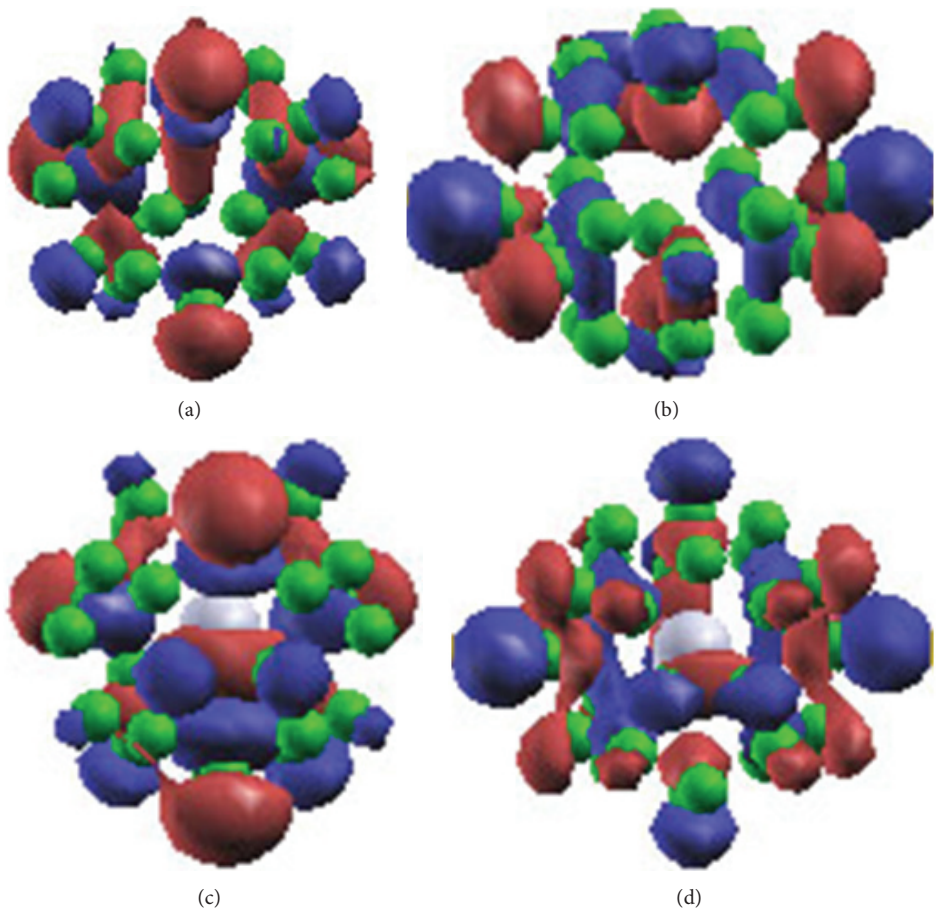

Figure 6: Molecular orbital occupation states of the two-probe system: (a) HOMO of Au-C_{28}-Au, (b) LUMO of Au-C_{28}-Au, (c) HOMO of Au-Li@C_{28}-Au, and (b) LUMO of Au-Li@C_{28}-Au.

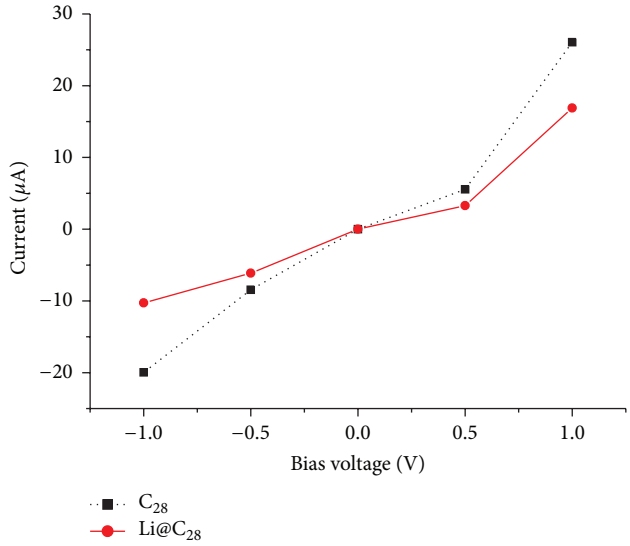

Figure 7: Current as a function of the bias voltage applied to the molecular junction formed by coupling of $Li@C_{28}$ (solid line) to Au electrodes. The current for C_{28} (dotted line) is also shown for comparison.

peaks in the bias window of transmission spectra represent hybridized molecular orbitals of the scattering region in presence of gold electrodes. Here, the transmission close to the Fermi energy appears to be dominated by HOMO of the molecule. For $Li@C_{28}$, a vanishing transmission near the Fermi region indicates a larger HOMO-LUMO gap. In the absence of any resonant peak, caused by a decrease in the degree of coupling between central cluster and electrodes, a lesser magnitude of current as compared to the pristine fullerene molecule is obtained.

Upon increasing the bias voltage to 1 V, there are more channels in the bias window contributing to the transmission, causing a further increase in current. While there are more and stronger conduction channels for undoped C_{28} molecule, a transmission valley appearing in Figure 4(f) suggests weak effective coupling of the $Li@C_{28}$ molecule with electrodes, which is also apparent in the smaller width of the transmission peaks.

The current-voltage characteristics of the molecular device formed by sandwiching undoped C_{28} cage and $Li@C_{28}$ cage, respectively, between two Au electrodes are shown in Figure 7. The current is found to increase with increase in bias voltage for all three molecular junctions. In general current increases nonlinearly with voltage. While a metal-like conduction is observed at small bias (−0.5 V to 0.5 V), a rapid increase in current occurs as the bias is further increased to 1 V. The increase in current for undoped C_{28} is more as compared to $Li@C_{28}$ molecule.

4. Conclusion

Endohedral doping of C_{28} with Li atom is found to affect its electronic structure and hence the transport properties. The electronic transport properties of doped fullerene $Li@C_{28}$ and host C_{28} molecule sandwiched between two gold surfaces have been calculated using first-principles density functional theory and nonequilibrium Green's function formalism. The transmission curves and IV characteristics of both pristine and doped molecule are computed. The current across the junction is found to decrease upon Li encapsulation. The change in current is more pronounced at higher voltage, which indicates that introduction of the dopant atom in C_{28} cage weakens the electron transport, and can be attributed to modification in alignment of the molecular orbitals in presence of electrodes.

Conflict of Interests

The authors declare that there is no conflict of interests regarding the publication of this paper.

References

[1] C. Joachim, J. K. Gimzewski, and A. Aviram, "Electronics using hybrid-molecular and mono-molecular devices," *Nature*, vol. 408, no. 6812, pp. 541–548, 2000.

[2] N. J. Tao, "Electron transport in molecular junctions," *Nature Nanotechnology*, vol. 1, pp. 173–181, 2006.

[3] A. Nitzan and M. A. Ratner, "Electron transport in molecular wire junctions," *Science*, vol. 300, no. 5624, pp. 1384–1389, 2003.

[4] M. A. Reed, C. Zhou, C. J. Muller, T. P. Burgin, and J. M. Tour, "Conductance of a molecular junction," *Science*, vol. 278, no. 5336, pp. 252–254, 1997.

[5] A. Aviram and M. A. Ratner, "Molecular rectifiers," *Chemical Physics Letters*, vol. 29, pp. 277–283, 1974.

[6] J. Chen, M. A. Reed, A. M. Rawlett, and J. M. Tour, "Large on-off ratios and negative differential resistance in a molecular electronic device," *Science*, vol. 286, no. 5444, pp. 1550–1552, 1999.

[7] J. Park, A. N. Pasupathy, J. I. Goldsmith et al., "Coulomb blockade and the Kondo effect in single-atom transistors," *Nature*, vol. 417, pp. 722–725, 2002.

[8] S. J. Tans, A. R. M. Verschueren, and C. Dekker, "Room-temperature transistor based on a single carbon nanotube," *Nature*, vol. 393, no. 6680, pp. 49–52, 1998.

[9] Y. Huang, X. Duan, Y. Cui, L. J. Lauhon, K.-H. Kim, and C. M. Lieber, "Logic gates and computation from assembled nanowire building blocks," *Science*, vol. 294, no. 5545, pp. 1313–1317, 2001.

[10] D. M. Eigler, C. P. Lutz, and W. E. Rudge, "An atomic switch realized with the scanning tunnelling microscope," *Nature*, vol. 352, no. 6336, pp. 600–603, 1991.

[11] I. Willner and B. Willner, "Biomaterials integrated with electronic elements: en route to bioelectronics," *Trends in Biotechnology*, vol. 19, no. 6, pp. 222–230, 2001.

[12] C. Joachim, J. K. Gimzewski, R. R. Schlittler, and C. Chavy, "Electronic transparence of a single C_{60} molecule," *Physical Review Letters*, vol. 74, no. 11, pp. 2102–2105, 1995.

[13] D. Porath and O. Millo, "Single electron tunneling and level spectroscopy of isolated C_{60} molecules," *Journal of Applied Physics*, vol. 81, no. 5, pp. 2241–2244, 1997.

[14] K. Xu, J. Huang, Z. Guan, Q. Li, and J. Yang, "Transport spin polarization of magnetic C_{28} molecular junctions," *Chemical Physics Letters*, vol. 535, pp. 111–115, 2012.

[15] J. Zhao, C. Zeng, X. Cheng et al., "Single $C_{59}N$ molecule as a molecular rectifier," *Physical Review Letters*, vol. 95, Article ID 045502, 2005.

[16] C. G. Zeng, H. Q. Wang, B. Wang, and J. L. Yang, "Negative differential-resistance device involving two C_{60} molecules," *Applied Physics Letters*, vol. 77, p. 3595, 2000.

[17] N. Neel, J. Kroger, L. Limot, and R. Berndt, "Conductance of oriented C60 molecules," *Nano Letters*, vol. 8, no. 5, pp. 1291–1295, 2008.

[18] S. Bilan, L. A. Zotti, F. Pauly, and J. C. Cuevas, "Theoretical study of the charge transport through C_{60} -based single-molecule junctions," *Physical Review B*, vol. 85, Article ID 205403, 2012.

[19] B. Abbaszadeh and M. D. Ganji, "Electrical characteristics of C_{36} molecular conductor and its B- and N-Doped isomers," *Electronic Materials Letters*, vol. 9, no. 2, pp. 63–69, 2013.

[20] X. Zhong, R. Pandey, A. R. Rocha, and S. P. Karna, "Can single-atom change affect electron transport properties of molecular nanostructures such as C_{60} fullerene?" *The Journal of Physical Chemistry Letters*, vol. 1, no. 10, pp. 1584–1589, 2010.

[21] Y. P. An, C. L. Yang, M. S. Wang, X. G. Ma, and D. H. Wang, "First-principles study of transport properties of endohedral $Li@C_{20}$ metallofullerene," *Current Applied Physics*, vol. 10, pp. 260–265, 2010.

[22] X. J. Zhang, M. Q. Long, K. Q. Chen et al., "Electronic transport properties in doped C_{60} molecular devices," *Applied Physics Letters*, vol. 94, Article ID 073503, 2009.

[23] T. Guo, M. D. Diener, Y. Chai et al., "Uranium stabilization of C_{28}: a tetravalent fullerene," *Science*, vol. 257, no. 5077, pp. 1661–1664, 1992.

[24] H. Funasaka, K. Sugiyama, K. Yamamoto, and T. Takahashi, "Synthesis of actinide carbides encapsulated within carbon nanoparticles," *Journal of Applied Physics*, vol. 78, no. 9, pp. 5320–5324, 1995.

[25] M. R. Pederson and N. Laouini, "Covalent container compound: empty, endohedral, and exohedral C28 complexes," *Physical Review B*, vol. 48, no. 4, pp. 2733–2737, 1993.

[26] K. Jackson, E. Kaxiras, and M. R. Pederson, "Electronic states of group-IV endohedral atoms in C_{28}," *Physical Review B*, vol. 48, no. 23, pp. 17556–17561, 1993.

[27] Z. Li, B. Gu, and R. Han, "Electronic properties of C_{28} and $Hf@C_{28}$ clusters," *Chemical Physics Letters*, vol. 207, pp. 41–44, 1993.

[28] T. Guo, R. E. Smalley, and G. Scuseria, "Ab initio theoretical predictions of C_{28}, $C_{28}H_4$, $C_{28}F_4$, $(Ti@C_{28})H_4$, and $M@C_{28}$ (M=Mg, Al, Si, S, Ca, Sc, Ti, Ge, Zr, and Sn)," *The Journal of Chemical Physics*, vol. 99, no. 1, p. 352, 1993.

[29] O. Hiroshi, "Preparation of endohedral fullerene containing lithium ($Li@C_{60}$) and isolation as pure hexafluorophosphate salt ($[Li^+@C_{60}][PF_6^-]$)," *RSC Advances*, vol. 2, no. 28, pp. 10624–10631, 2012.

[30] S. Aoyagiet, E. Nishibori, H. Sawa et al., "A layered ionic crystal of polar $Li@C_{60}$ superatoms," *Nature Chemistry*, vol. 2, pp. 678–683, 2010.

[31] J. M. Soler, E. Artacho, J. D. Gale et al., "The SIESTA method for ab initio order-N materials simulation," *Journal of Physics Condensed Matter*, vol. 14, no. 11, pp. 2745–2779, 2002.

[32] D. M. Ceperley and B. J. Alder, "Ground state of the electron gas by a stochastic method," *Physical Review Letters*, vol. 45, no. 7, pp. 566–569, 1980.

[33] N. Troullier and J. L. Martins, "Efficient pseudopotentials for plane-wave calculations," *Physical Review B*, vol. 43, p. 1993, 1991.

[34] M. Brandbyge, J. L. Mozos, P. Ordejon, J. Taylor, and K. Stokbro, "Density-functional method for nonequilibrium electron transport," *Physical Review B*, vol. 65, no. 16, Article ID 165401, 17 pages, 2002.

[35] M. Büttiker, Y. Imry, R. Landauer, and S. Pinhas, "Generalized many-channel conductance formula with application to small rings," *Physical Review B*, vol. 31, no. 10, pp. 6207–6215, 1985.

[36] H. J. Monkhorst and J. D. Pack, "Special points for Brillouin-zone integrations," *Physical Review. B. Solid State*, vol. 13, no. 12, pp. 5188–5192, 1976.

[37] K. Jackson, E. Kaxiras, and M.-R. Pederson, "Bonding of endohedral atoms in small carbon fullerenes," *Journal of Physical Chemistry*, vol. 98, no. 32, pp. 7805–7810, 1994.